Favorable Biokinetic and Tumor-Targeting Properties of ^{99m}Tc-Labeled Glucosamino RGD and Effect of Paclitaxel Therapy

Kyung-Ho Jung[1], Kyung-Han Lee[1], Jin-Young Paik[1], Bong-Ho Ko[1], Jun-Sang Bae[1], Byung Chul Lee[2], Hyun Ju Sung[2], Dong Hyun Kim[1], Yearn Seong Choe[1], and Dae Yoon Chi[2]

[1]Department of Nuclear Medicine, Samsung Medical Center, Sungkyunkwan University School of Medicine, Seoul, Korea; and [2]Department of Chemistry, Inha University, Inchun, Korea

Compared with the recent advancements in radiohalogenated Arg-Gly-Asp (RGD) peptides for $\alpha_v\beta_3$-targeted imaging, there has been limited success with ^{99m}Tc-labeled RGD compounds. In this article, we describe the favorable in vivo kinetics and tumor-imaging properties of a novel ^{99m}Tc-RGD compound that contains a glucosamine moiety. **Methods:** Glucosamino ^{99m}Tc-D-c(RGDfK) was prepared by incorporating ^{99m}Tc(CO)$_3$ to the glucosamino peptide precursor in high radiochemical yield. Cell-binding characteristics were tested on human endothelial cells. Mice bearing RR1022 fibrosarcoma and Lewis lung carcinoma (LLC) tumors were used for in vivo biodistribution and blocking experiments and for imaging studies. Separate LLC-bearing mice underwent antiangiogenic therapy with 0, 20, or 40 mg of paclitaxel per kilogram of body weight every 2 d. Tumor volume was serially monitored, and tumor glucosamino ^{99m}Tc-D-c(RGDfK) uptake and Western blots of α_v integrin expression were analyzed at day 14. **Results:** Glucosamino ^{99m}Tc-D-c(RGDfK) binding to endothelial cells was dose-dependently inhibited by excess RGD. Biodistribution in mice showed rapid blood clearance of glucosamino ^{99m}Tc-D-c(RGDfK), with substantially lower liver uptake and higher tumor uptake compared with ^{125}I-c(RGD(I)yV). Tumor uptake was 1.03 ± 0.21 and 1.18 ± 0.26 %ID/g at 1 h and 0.85 ± 0.05 and 0.89 ± 0.28 %ID/g at 4 h for sarcomas and carcinomas, respectively. Excess RGD blocked uptake by 76.5% and 70.2% for the respective tumors. γ-Camera imaging allowed clear tumor visualization, with an increase of sarcoma-to-thigh count ratios from 5.5 ± 0.7 at 1 h to 10.1 ± 2.2 at 4 h and sustained carcinoma-to-thigh count ratios from 4 to 17 h. Pretreatment with excess cRGDyV significantly reduced tumor contrast on images. Paclitaxel therapy in LLC tumor–bearing mice significantly retarded tumor growth. This was accompanied by a corresponding reduction of tumor glucosamino ^{99m}Tc-D-c(RGDfK) uptake, which correlated significantly with tumor α_v integrin expression levels. **Conclusion:** Glucosamino ^{99m}Tc-D-c(RGDfK) has favorable in vivo biokinetics and tumor-imaging properties and may be useful for noninvasive evaluation of tumor integrin expression and response to antiangiogenic therapeutics. Because of the wide accessibility of γ-cameras and high availability and excellent imaging characteristics of ^{99m}Tc, glucosamino ^{99m}Tc-D-c(RGDfK) may be an attractive alternative to radiohalogenated RGD peptides for angiogenesis-imaging research.

Key Words: RGD peptide; ^{99m}Tc; integrin; tumor; angiogenesis; paclitaxel

Targeting of tumor angiogenesis–related receptors is a promising approach to advancing cancer diagnosis and treatment. $\alpha_v\beta_3$ integrin is a receptor that mediates cellular interaction with the extracellular matrix and is a key mediator of tumor growth (1), local invasiveness (2), metastatic potential (3), and angiogenesis (4). As such, antagonists against $\alpha_v\beta_3$ integrin are being evaluated as a strategy for tumor-specific anticancer therapy (5,6) and for targeting a variety of therapeutic agents to tumor tissue (7,8). Based on the discovery that the tripeptide Arg-Gly-Asp (RGD) sequence serves as a specific binding motif for integrin receptors, various RGD analogs have been developed as $\alpha_v\beta_3$ antagonists (9,10) and as radiolabeled tracers for noninvasive angiogenesis imaging (11–15).

Since the introduction of ^{125}I-3-iodo-Tyr^4-cyclo(-Arg-Gly-Asp-D-Tyr-Val-) (^{125}I-c(RGD(I)yV)) as a first-generation radiotracer (11), there have been significant advancements in radiolabeled RGD compounds, including conjugation of glycosylated moieties to reduce hepatic uptake and biliary excretion (12), radiolabeling with positron emitters to allow imaging with PET (13,14), and insertion of poly(ethylene glycol) moieties to improve in vivo kinetics (15,16).

Another significant advancement that would facilitate the widespread application of RGD imaging is the establishment of a satisfactory ^{99m}Tc-labeled compound to allow convenient monitoring with widely available γ-cameras and the easily accessible radionuclide. To date, however, there has been only limited success in the development of a ^{99m}Tc-labeled RGD compound with

sufficient in vivo biokinetics and tumor angiogenesis–imaging properties. Su et al. synthesized a ^{99m}Tc-labeled RGD-4C peptide hydrazinonicotinamide (HYNIC) conjugate, but its target affinity was insufficient to allow significant accumulation in murine tumors ([17]). Janssen et al. developed a ^{99m}Tc-labeled compound containing 2 cyclo(RGDfK) loops and a single HYNIC moiety (^{99m}Tc-HYNIC-E-[c(RGDfK)]$_2$) that achieved high maximum tumor uptake in a mouse model. However, this was accompanied by undesirable biokinetic properties, including substantial hepatic and splenic uptake and also excessive renal retention presumably due to a high positive charge ([18]). Haubner et al. synthesized ^{99m}Tc-N$^\varepsilon$-(H-Asp-Lys-Cys-Lys)-Lys^5-cyclo(-Arg-Gly-Asp-D-Phe-Lys-), which was taken up by $\alpha_v\beta_3$-positive tumors but was limited in usefulness because of metabolic instability and prolonged kidney retention ([19]).

We, in collaboration with another group, have recently developed a novel ^{99m}Tc-labeled RGD compound that contains N-D-glucosamine as a sugar moiety (glucosamino ^{99m}Tc-D-c(RGDfK)) and have confirmed its high affinity and specific binding to $\alpha_v\beta_3$ integrin in vitro (submitted elsewhere). In this study, we investigated the in vivo kinetics and imaging properties of glucosamino ^{99m}Tc-D-c(RGDfK) using mice bearing carcinoma and sarcoma tumors.

MATERIALS AND METHODS

Synthesis of Glucosamino ^{99m}Tc-D-c(RGDfK) and ^{125}I-c(RGD(I)yV)

The details of the procedures for synthesis of glucosamino ^{99m}Tc-D-c(RGDfK) (Fig. 1A) have been reported and submitted elsewhere ([20]). Briefly, ^{99m}Tc-D-c(RGDfK) was prepared by reacting glucosamino [N-α-bis(hydroxycarbonylmethyl)-G]-D-c(RGDfK) with [^{99m}Tc(H$_2$O)$_3$(CO)$_3$]$^+$ in a mixture of methanol and water at 65°C for 30 min, followed by purification with high-performance liquid chromatography (HPLC). The desired fraction of the radiotracer was collected from HPLC, and the HPLC solvent was partly removed under a gentle stream of N$_2$. The residue was loaded onto a C18 Sep-Pak cartridge (Waters), which was washed with 10 mL of H$_2$O and

then with 2 mL of methanol. The methanol fraction was dried under a stream of N$_2$ and diluted with D-PBS (pH 7.4).

^{125}I-c(RGD(I)yV) was synthesized by following previously described procedures ([11]) and was used for comparison of biokinetic properties.

Cell-Binding Experiment

Human umbilical vein endothelial cells (American Type Culture Collection [ATCC]) were cultured at 37°C and 5% CO$_2$ in endothelial cell basal medium 2 containing endothelial growth supplements, 12% fetal bovine serum, and antibiotics. Cells of 80%–90% confluence were harvested with trypsin and washed twice with Dulbecco's phosphate-buffered saline, and 10^6 cells were transferred to Eppendorf tubes. After incubation with 37 kBq of glucosamino ^{99m}Tc-D-c(RGDfK) in Dulbecco's phosphate-buffered saline (which contains a 0.5 mmol/L concentration of MgCl$_2$ and a 0.9 mmol/L concentration of CaCl$_2$) at 37°C and 5% CO$_2$ for 1 h, the cells were rapidly washed twice with Dulbecco's phosphate-buffered saline and measured for bound radioactivity on a γ-counter. The specificity of endothelial binding was evaluated by competitive binding experiments in the presence of 0, 1, 10, 100, or 1,000 nmol/L or 10 μmol/L of the standard peptide cRGDyV. Binding to cultured RR1022 cells and Lewis lung carcinoma (LLC) cells was also evaluated in the presence of 0, 0.1, 1, or 10 μmol/L of cRGDyV using a method identical to that for endothelial cells.

Preparation of Tumor-Bearing Mice

All animal studies were performed under protocols approved by the Institution Guidelines on the Use and Care of Animals. Two types of murine tumor models were used for the in vivo biodistribution and imaging studies. RR1022 rat fibrosarcoma cells (ATCC) were maintained in RPMI 1640 medium (Gibco BRL), and LLC (ATCC) cells established from mouse lung cancer were maintained in Dulbecco's modified Eagle medium (Gibco BRL) at 37°C in 5% CO$_2$. Both media were supplemented with 10% fetal bovine serum, 2 mmol of glutamine per liter, 100 U of penicillin per milliliter, and 100 mg of streptomycin per liter. RR1022 and LLC tumors were grown in male in BALB/C nude mice and C57BL6 mice, respectively, by subcutaneous injection of 10^9 tumor cells into the right flank. Biodistribution and imaging studies were performed when tumor diameter reached approximately 3 cm for the sarcomas and 2 cm for the carcinomas.
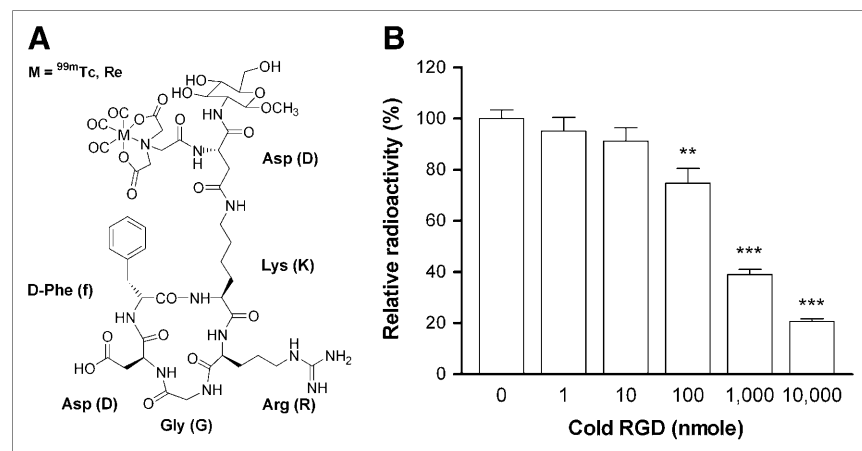

FIGURE 1. (A) Schematic structure of glucosamino ^{99m}Tc-D-c(RGDfK). (B) Competitive binding of glucosamino ^{99m}Tc-D-c(RGDfK) to human umbilical endothelial cells. Cell-binding levels are expressed as percentage relative to that in absence of nonradiolabeled cRGDyV. Results are mean ± SD of triplicate samples obtained from single experiment representative of 2 separate experiments. **$P < 0.05$ compared with controls. ***$P < 0.001$ compared with controls.

Biodistribution Studies

We first investigated the biodistribution of glucosamino ^{99m}Tc-D-c(RGDfK) in mice bearing either RR1022 sarcoma or LLC carcinoma tumors. RR1022-bearing mice received 3.1 MBq of glucosamino ^{99m}Tc-D-c(RGDfK) injected via the tail vein and were sacrificed 1 or 4 h later ($n = 3$ for each group). LLC-bearing mice received 3.7 MBq of glucosamino ^{99m}Tc-D-c(RGDfK) (28 MBq for the 17-h group) and were sacrificed 1, 4, or 17 h later ($n = 5$ for each group). Blood and major organs were promptly extracted and measured for ^{99m}Tc radioactivity on a high-energy γ-counter (Wallac).

The specificity of tumor uptake was investigated by pre-injecting an excess dose of nonradiolabeled cRGDyV 10 min before glucosamino ^{99m}Tc-D-c(RGDfK) administration. Two RR1022 tumor–bearing mice and 5 LLC tumor–bearing mice were preinjected with 9 and 15 mg, respectively, of cRGDyV per kilogram of body weight, and the accumulation of glucosamino ^{99m}Tc-D-c(RGDfK) at 4 h in the blood, muscle, and tumor in these animals was compared with that in control animals.

In addition, we compared the biodistributions of glucosamino ^{99m}Tc-D-c(RGDfK) and ^{125}I-c(RGD(I)yV) in the RR1022 sarcoma–bearing mice used for the biodistribution study as above. These animals received a 0.37 MBq injection of ^{125}I-c(RGD(I)yV) simultaneously with the glucosamino ^{99m}Tc-D-c(RGDfK) administration. After the animals had been sacrificed 1 or 4 h later ($n = 3$ each) and major organs and tumors had been measured for ^{99m}Tc radioactivity, the tissues were left for 3 d to allow the ^{99m}Tc to decay and then were measured for ^{125}I radioactivity on a conventional γ-counter.

γ-Camera Imaging of Tumor-Bearing Mice

RR1022 sarcoma–bearing mice used for the 4-h biodistribution study underwent scintigraphic imaging at 1 and 4 h after injection of glucosamino ^{99m}Tc-D-c(RGDfK). LLC carcinoma–bearing mice used for the 17-h biodistribution study underwent scintigraphy at 4 and 17 h after injection. To assess the specificity of image-based tumor uptake, RR1022-bearing mice injected with 0 or 9 mg of cRGDyV per kilogram 10 min before glucosamino ^{99m}Tc-D-c(RGDfK) administration underwent scintigraphic imaging at 1 and 4 h after injection.

Images were acquired using a γ-camera (Monad XLT; Trionix Research Laboratory) equipped with a pinhole collimator. A 15% energy window centered around 140 keV was used, and data were stored on a matrix of 256×256 pixels. For semiquantification of image-based uptake levels, 7×7 pixel square regions of interest were placed on the tumors and contralateral thigh region, from which tumor-to-thigh count ratios were measured.

Paclitaxel Effect on Tumor Size and Glucosamino ^{99m}Tc-D-c(RGDfK) Uptake

The effect of antiangiogenic therapy on tumor uptake of glucosamino ^{99m}Tc-D-c(RGDfK) was investigated by submitting LLC tumor–bearing C57BL6 mice to paclitaxel chemotherapy. Intraperitoneal paclitaxel therapy was initiated when tumors reached a diameter of about 10 mm, approximately 4 wk after subcutaneous injection of 1×10^6 cells, and a dose of 20 mg/kg ($n = 7$) or 40 mg/kg ($n = 7$) was injected for a total of 6 doses at 2-d intervals. On the same days, control animals ($n = 7$) received an injection of dilution buffer that did not contain paclitaxel. Immediately before each round of treatment, each animal was measured for body weight and tumor volume. Tumor volume was calculated from caliper measurements of the length and width of the masses using the equation suggested by Gutman et al. (21): volume (mm^3) = length × width^2 × ½. The relative tumor volume was calculated as the volume at a given time divided by the volume on the second day after the initiation of treatment.

One day after the final round of paclitaxel therapy, the mice received a 0.83 MBq intravenous injection of glucosamino ^{99m}Tc-D-c(RGDfK) and were sacrificed 4 h later. The tumors were promptly dissected, weighed, and measured for radioactivity, and uptake levels were expressed as the mean (±SD) of the percentage injected dose per gram of tissue (%ID/g). These tissues were then snap-frozen and stored at $-70°$C until used for Western blotting.

Western Blotting of Tumor $α_v$ Integrin Expression

Tumor tissue obtained from paclitaxel-treated and control animals was homogenized and extracted with PRO-PREP Protein Extraction Solution (iNtRON Biotechnology, Inc.). Protein concentration was determined according to the Bradford method. Proteins were separated by 10% sodium dodecyl sulfate (SDS) polyacrylamide gel electrophoresis (PAGE) under reducing conditions and transferred onto electroblotted polyvinylidene difluoride membranes. After incubation with a polyclonal rabbit anti-$α_v$ antibody (1:100 dilution; CHEMICON International) for 1 h followed by incubation with a secondary antibody, the immunoreactive proteins were detected with an enhanced chemiluminescence detection system. The protein band intensities were then measured using a GS-800 calibrated densitometer and Quantity One software (Bio-Rad Laboratories).

Data Analysis

Cell-binding experiments were repeated 2 separate times, and the results from a single representative experiment using triplicate samples were presented. Results were expressed as the mean (±SD) percentage uptake relative to controls, and the Student t test was used to evaluate the statistical significance of differences between groups. The significance of differences in tumor or organ uptake between groups in the biodistribution studies, and of differences in tumor volume during paclitaxel therapy, was assessed by the Student t test. P values of less than 0.05 were considered significant. The relationship between tumoral radiotracer uptake (%ID/g) and relative $α_v$ integrin expression in animals treated with paclitaxel was assessed by linear correlation.

RESULTS

Binding to Cultured Endothelial Cells and Tumor Cells

On competitive binding experiments, human umbilical endothelial cell binding of glucosamino ^{99m}Tc-D-c(RGDfK) was inhibited by excess cRGDyV peptide in a dose-dependent manner. Of the doses tested, the presence of a 10 μmol/L concentration of cRGDyV led to maximal blocking of radiotracer uptake to 20.7% ± 1.0% of control levels ($P < 0.0001$), indicating that the majority of glucosamino ^{99m}Tc-D-c(RGDfK) uptake corresponded to specific cellular binding (Fig. 1B). Uptake in

LLC cells was unaffected by excess cRGDyV, indicating the absence of specific tracer binding. Uptake in RR1022 cells was reduced by a 10 μmol/L concentration of cRGDyV to 55.8% ± 10.7% of control levels ($P < 0.05$), suggesting a certain amount of specific binding of glucosamino ^{99m}Tc-D-c(RGDfK) to these cells.

Biodistribution Studies

Biodistribution data on glucosamino ^{99m}Tc-D-c(RGDfK) in RR1022 sarcoma–bearing BALB/C nude mice and LLC carcinoma–bearing C57BL6 mice are summarized in Table 1. In both tumor models, 1-h uptake was highest in the kidneys, ranging from 3.3 to 4.6 %ID/g, but renal activity was rapidly reduced by 4 h, indicating renal excretion without significant retention of the radiotracer. Liver uptake for the 2 tumor models ranged from 2.0 to 2.5 %ID/g at 1 h and 0.5 to 1.4 %ID/g at 4 h. The absence of an increase in intestinal activity over time for the LLC model indicates that the radiotracer does not undergo significant biliary excretion. RR1022 sarcomas and LLC carcinomas demonstrated similar levels of glucosamino ^{99m}Tc-D-c(RGDfK) accumulation, which reached 1.03 and 1.18 %ID/g at 1 h and 0.85 and 0.89 %ID/g at 4 h, respectively. Blood and skeletal muscle uptake was similarly low at 4 h and resulted in tumor-to-blood ratios of 4.4 for both tumor types, and tumor-to-muscle ratios of 5.2 and 4.8 for RR1022 and LLC tumors, respectively. At 17 h, uptake in LLC tumors remained relatively high at 0.56 %ID/g, resulting in tumor-to-blood and tumor-to-muscle ratios of 4.7 and 6.0, respectively.

In vivo blocking studies with excess cRGDyV resulted in significantly reduced 4-h uptake of glucosamino ^{99m}Tc-D-c(RGDfK) for both tumor types. Tumor uptake was decreased from 1.81 ± 0.39 to 0.43 ± 0.10 %ID/g for RR1022 sarcomas ($P < 0.05$) and from 0.89 ± 0.28 to 0.27 ± 0.12 %ID/g for LLC carcinomas ($P < 0.005$; Fig. 2). This represents 76.5% and 70.2% reductions of tumor uptake for the respective tumor types. In contrast, radiotracer activities in blood and skeletal muscle were not significantly influenced by the presence of excess cRGDyV (Fig. 2).

A comparison of biodistribution patterns for glucosamino ^{99m}Tc-D-c(RGDfK) and ^{125}I-c(RGD(I)yV) coinjected into RR1022 sarcoma–bearing BALB/C nude mice is shown in Figure 3. Clearance of blood activity was more rapid for glucosamino ^{99m}Tc-D-c(RGDfK). ^{125}I-c(RGD(I)yV) showed substantially higher liver uptake and higher stomach and thyroid uptake indicative of dehalogenation of the radioiodine label. Tumor uptake was significantly higher for glucosamino ^{99m}Tc-D-c(RGDfK) at both 1 and 4 h after injection, with a substantially greater 4-h tumor-to-blood ratio of 4.4 ± 0.2, compared with 0.6 ± 0.1 for ^{125}I-c(RGD(I)yV).

γ-Camera Imaging

γ-Camera imaging demonstrated renal excretion of glucosamino ^{99m}Tc-D-c(RGDfK), with accumulation in the bladder. Biliary and intestinal activity was negligible, and thyroid uptake was not visible. RR1022 sarcomas were clearly visualized at 1 and 4 h after radiotracer injection (Fig. 4A), and region-of-interest–based tumor-to-thigh count ratios increased from 5.5 ± 0.7 to 10.1 ± 2.2 during this time frame ($P < 0.05$). LLC carcinomas were also visualized with high contrast at 4 and 17 h after injection, without a significant change in tumor-to-thigh count ratios (from 9.8 ± 4.9 to 9.2 ± 4.4). RR1022 tumor–bearing mice pretreated with a 9 mg/kg dose of nonradiolabeled cRGDyV demonstrated significantly reduced tumor contrast (Fig. 4B) and lower tumor-to-thigh count ratios, compared with controls, at 1 h (4.6 ± 0.1 vs. 1.5 ± 0.3, $P < 0.01$) and 4 h (5.7 ± 0.2 to 2.8 ± 0.3, $P < 0.01$) after glucosamino ^{99m}Tc-D-c(RGDfK) injection.

TABLE 1
Biodistribution of Glucosamino ^{99m}Tc-D-c(RGDfK) in RR1022 Fibrosarcoma–Bearing BALB/C Nude Mice and LLC-Bearing C57Bl6 Mice

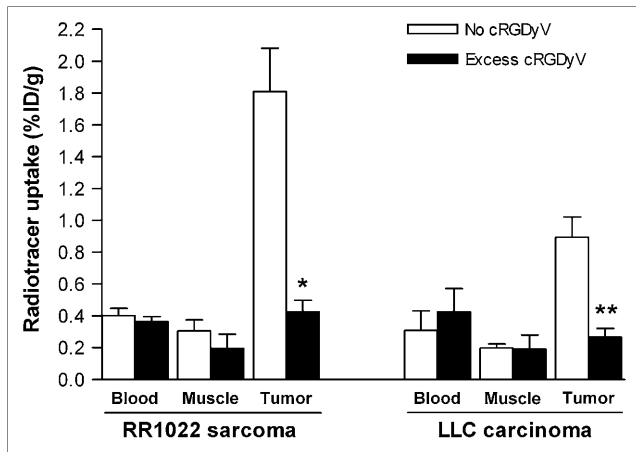| Tissue	RR1022 fibrosarcoma		LLC		
	1 h ($n = 3$)	4 h ($n = 3$)	1 h ($n = 5$)	4 h ($n = 5$)	17 h ($n = 5$)
Blood	0.50 ± 0.01	0.19 ± 0.02	1.19 ± 0.44	0.19 ± 0.02	0.12 ± 0.06
Heart	0.53 ± 0.09	0.21 ± 0.02	0.94 ± 0.30	0.23 ± 0.04	0.15 ± 0.07
Lung	1.59 ± 0.17	0.63 ± 0.11	2.76 ± 0.77	0.66 ± 0.15	0.38 ± 0.17
Liver	1.99 ± 0.22	1.43 ± 0.15	2.49 ± 0.69	0.51 ± 0.15	0.87 ± 0.57
Spleen	0.72 ± 0.09	0.32 ± 0.02	2.05 ± 0.74	0.41 ± 0.07	0.27 ± 0.14
Kidney	3.33 ± 1.14	1.76 ± 0.10	4.60 ± 1.32	1.61 ± 0.23	1.66 ± 0.80
Stomach	1.77 ± 0.33	0.94 ± 0.31	2.09 ± 1.02	1.20 ± 0.59	1.12 ± 0.61
Intestine	—	—	3.22 ± 2.39	1.62 ± 0.63	0.73 ± 0.46
Thyroid	1.67 ± 1.27	0.34 ± 0.01	2.89 ± 3.04	0.88 ± 0.51	0.43 ± 0.21
Muscle	0.85 ± 0.43	0.17 ± 0.07	0.74 ± 0.33	0.20 ± 0.05	0.09 ± 0.04
Tumor	1.03 ± 0.21	0.85 ± 0.05	1.18 ± 0.26	0.89 ± 0.28	0.56 ± 0.30

Data are mean ± SD of %ID/g.

FIGURE 2. Inhibition study of tumor glucosamino ^{99m}Tc-D-c(RGDfK) accumulation. LLC- and RR1022 fibrosarcoma–bearing mice that received intravenous injection of glucosamino ^{99m}Tc-D-c(RGDfK) in absence or presence of excess nonradiolabeled cRGDyV were sacrificed 4 h later and measured for blood, muscle, and tumor uptake. Data are shown as mean ± SD of 5 and 2 animals per each carcinoma and sarcoma group, respectively. *$P < 0.05$ compared with corresponding uninhibited group. **$P < 0.005$ compared with corresponding uninhibited group.

Effect of Paclitaxel Therapy on Radiouptake and Correlation to α_v Integrin Expression

LLC tumor–bearing mice treated with paclitaxel demonstrated a dose-dependent retardation of tumor growth, compared with control animals (Fig. 5A). Tumor volume ratios at 13 d after the initiation of therapy were 21.3 ± 4.4, 17.4 ± 5.9, and 13.2 ± 4.4 for animals injected with 0, 20, and 40 mg, respectively, of paclitaxel

per kilogram ($P < 0.01$ between the 0 and 40 mg/kg groups). In a similar fashion, 3-h tumor uptake levels of glucosamino ^{99m}Tc-D-c(RGDfK) were significantly lower for animals treated with a 40 mg/kg dose of paclitaxel (0.69 ± 0.21 %ID/g) than for controls (1.05 ± 0.27 %ID/g, $P < 0.05$; Fig. 5B).

When the radiouptake in %ID/g and the intensity of protein bands on Western blots were compared, a significant correlation was found between glucosamino ^{99m}Tc-D-c(RGDfK) uptake levels and the magnitude of α_v integrin expression in the tumor tissue ($r = 0.44$, $P < 0.05$; Fig. 5C).

DISCUSSION

In this study, we investigated the biokinetics and tumor-targeting characteristics of glucosamino ^{99m}Tc-D-c(RGDfK), a novel sugar moiety containing ^{99m}Tc-labeled RGD compound. In vitro experiments showed specific binding to cultured human endothelial cells that was dose-dependently inhibited by nonradiolabeled RGD. Biodistribution studies revealed favorable in vivo biokinetic properties, with significant levels of receptor-specific tumor uptake, and imaging results demonstrated high-contrast visualization of both carcinomas and sarcomas. Furthermore, retardation of tumor growth induced by paclitaxel therapy was accompanied by a reduction of tumoral glucosamino ^{99m}Tc-D-c(RGDfK) accumulation, which correlated in extent to integrin expression levels.

To our knowledge, glucosamino ^{99m}Tc-D-c(RGDfK) is the first reported ^{99m}Tc-labeled RGD compound that contains a sugar moiety. Conjugation of glucosamine to
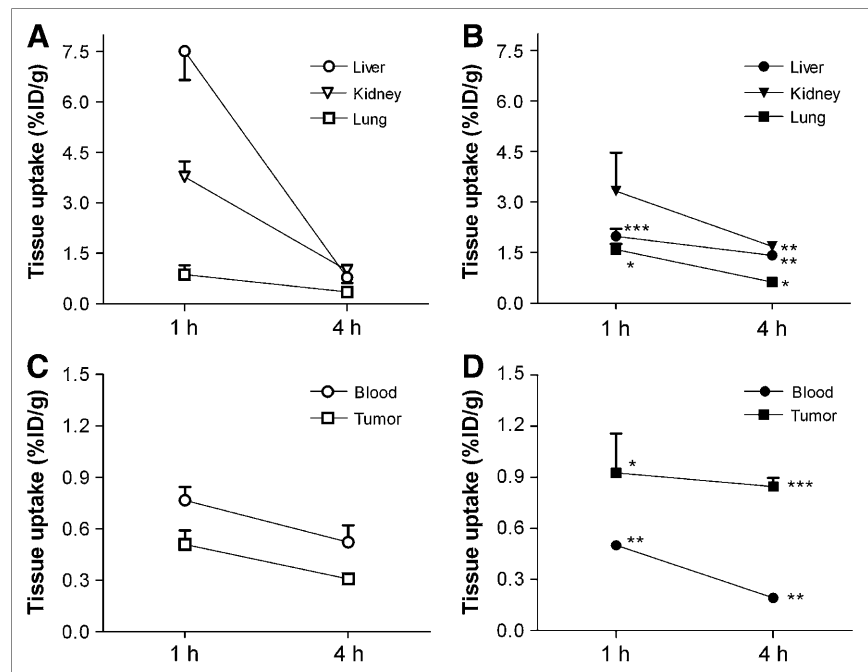

FIGURE 3. Comparison of biokinetic characteristics. Uptake levels of ^{125}I-c(RGD(I)yV) (A and C) and glucosamino ^{99m}Tc-D-c(RGDfK) (B and D) in major organs at 1 and 4 h after coinjection into same RR1022 sarcoma–bearing nude mice. Data are shown as mean ± SD of 3 animals. *$P < 0.05$ compared with ^{125}I-c(RGD(I)yV). **$P < 0.01$ compared with ^{125}I-c(RGD(I)yV). ***$P < 0.001$ compared with ^{125}I-c(RGD(I)yV).

A
RR1022 fibrosarcoma

1 h   4 h

LLC

4 h   17 h

B
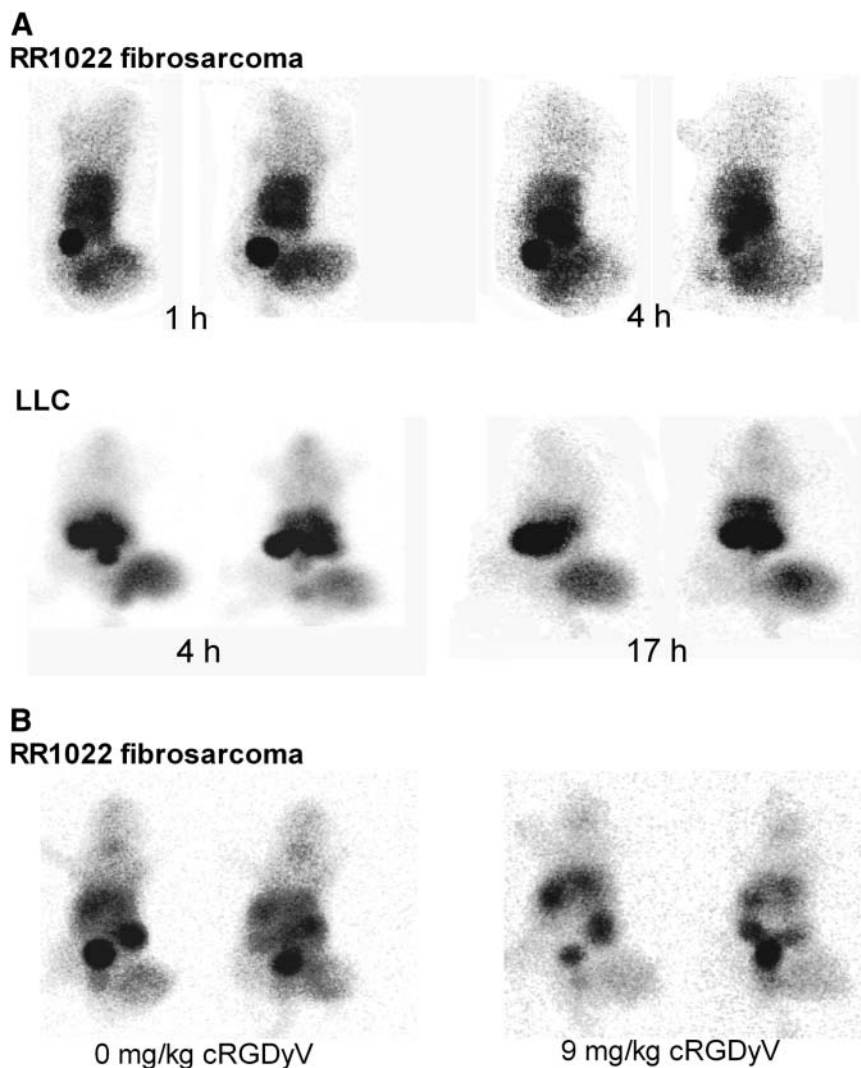### RR1022 fibrosarcoma

0 mg/kg cRGDyV   9 mg/kg cRGDyV

FIGURE 4. Scintigraphic pinhole images of tumor-bearing mice. (A) RR1022 fibrosarcoma and LLC tumors on right flank of BALB/C nude mice and C57Bl6 mice are clearly visualized after intravenous injection with glucosamino ^{99m}Tc-D-c(RGDfK). (B) RR1022 fibrosarcoma–bearing mice demonstrate appreciably reduced tumor visualization at 4 h when radiotracer is co-injected with nonradiolabeled cRGDyV.

aspartic acid linked to the lysine residue was possible without a significant reduction in binding affinity as confirmed by an inhibitory concentration of 50% of 80 nmol/L for binding to purified $\alpha_v\beta_3$ integrins (submitted elsewhere). Conjugation of sugar moieties as for this compound is a general strategy to enhance water solubility and reduce metabolic degradation of peptides. For example, whereas the first-generation ^{125}I-c(RGD(I)yV) was found to have undesirable high hepatic uptake and biliary excretion (11), the subsequently developed sugar amino acid conjugated ^{125}I-c(RGD(I)yK(SAA)) showed reduced hepatic uptake and improved biokinetic properties (12). Consistent with these reports, we observed prominent differences between the biodistribution of glucosamino ^{99m}Tc-D-c(RGDfK) in sarcoma-bearing nude mice and that of simultaneously injected ^{125}I-c(RGD(I)yV). Namely, glucosamino ^{99m}Tc-D-c(RGDfK) had substantially lower early hepatic and intestinal activity and significantly higher tumor uptake that resulted in greater tumor-to-

nontumor uptake ratios. Tumor accumulation of the radiotracer at 4 h approximated 0.9 %ID/g for both carcinomas and sarcomas, a value that was 4.5-fold and 5.0-fold higher than blood and muscle activity for sarcomas and 4.4-fold and 4.8-fold higher for carcinoma tumors. These tumor accumulation levels are at least as high as the 4-h uptake levels of 0.2–0.5 %ID/g previously reported for ^{125}I-c(RGD(I)yK(SAA)) (12). In comparison, the ^{99m}Tc-labeled RGD analog synthesized by Su et al. had a 6-h tumor uptake of 0.75 %ID/g, with a tumor-to-muscle ratio of 2.2 (17). The ^{99m}Tc tracer developed by Janssen et al. had a high 1-h tumor uptake of 6.0 %ID/g and a tumor-to-muscle ratio approximating 5.0, but with substantial uptake also in the liver, spleen, and kidneys (18). The ^{99m}Tc RGD peptide introduced by Haubner et al. showed a 4-h uptake of 1.1 %ID/g for $\alpha_v\beta_3$ integrin–positive melanoma tumors—a value that was 10-fold higher than muscle activity (19). To the best of our knowledge, whether RR1022 and LLC cells express or do not express $\alpha_v\beta_3$ integrin is not
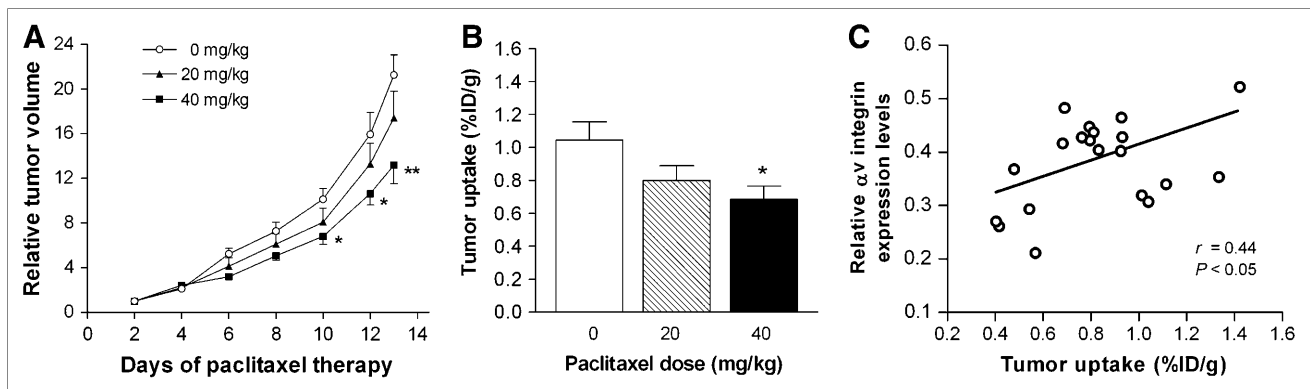
FIGURE 5. Effect of paclitaxel therapy. (A) Relative tumor volume of LLC during repeated administration of 0, 20, or 40 mg of paclitaxel per kilogram. Data are mean ± SD of measurements obtained from 7 animals per group. Tumor volume was calculated from caliper measurements of length and width of masses: volume (mm^3) = length × width^2 × ½. Relative tumor volume was calculated as volume at a given time divided by volume on second day after initiation of treatment. *$P < 0.05$ compared with control group. **$P < 0.01$ compared with control group. (B) Tumor uptake of glucosamino ^{99m}Tc-D-c(RGDfK) at 4 h on day 14 of paclitaxel therapy. Data are expressed as mean ± SD of %ID/g obtained from 7 animals per group. *$P < 0.05$ compared with control group. (C) Correlation between tumor glucosamino ^{99m}Tc-D-c(RGDfK) uptake expressed as %ID/g and α_v integrin levels on day 14 of paclitaxel therapy. α_v integrin levels were measured by Western blot of protein from homogenized tumor tissue using anti-α_v antibody and chemiluminescence system. Protein band intensities were measured by a calibrated densitometer and quantification software and are expressed in arbitrary units.

well established. Our in vitro experiments indicate that although its presence appears insignificant for LLC cells, some specific binding was shown for RR1022 cells, suggesting that in addition to endothelial binding, cancer cell binding may also have partly contributed to the RR1022 tumor radiouptake in vivo.

γ-Camera images showed kidney and bladder activity that indicates predominantly renal elimination of glucosamino ^{99m}Tc-D-c(RGDfK). The biodistribution data, however, indicate that renal activity is substantially reduced over 1–4 h after injection. The relatively low blood and muscle activity with reasonably high tumor uptake of glucosamino ^{99m}Tc-D-c(RGDfK) allowed clear imaging of both carcinoma and sarcoma tumors, with tumor-to-nontumor ratios that peaked at 4 h and were sustained up to 17 h after injection.

Although several previous radiolabeled RGD compounds have also shown encouraging tumor-targeting and -imaging properties, a more crucial determinant for a successful RGD radiotracer would be its ability to monitor the response of tumors to antiangiogenic therapeutics. In our study, anticancer therapy was performed using paclitaxel, an antimicrotubule agent and potent inhibitor of angiogenesis that is commonly used in the treatment of advanced breast, ovarian, and non–small cell lung carcinoma (22,23). LLC tumor–bearing mice treated with paclitaxel had a modest but significant retardation of tumor growth, compared with control animals. The modest effect of paclitaxel in our study may partly be related to the poor solubility of the drug in the small volume that was used for injection and may also be explained by the fact that, as a P-glycoprotein substrate, paclitaxel may have limited efficacy against

LLC tumors when used as a single agent (24). Notwithstanding these factors, however, paclitaxel did significantly retard tumor growth, and this retardation was accompanied by a significant reduction of tumor uptake of glucosamino ^{99m}Tc-D-c(RGDfK), suggesting that this radiotracer may be useful for monitoring tumor response to angiogenesis-targeted therapeutics.

Another important issue for RGD radiotracers is whether their extent of tumor accumulation actually reflects the level of tumor integrin expression. In this study, we confirmed a significant correlation between glucosamino ^{99m}Tc-D-c(RGDfK) uptake and protein bands of α_v integrin in tumor tissue, suggesting that the radiotracer may be useful for evaluating the amount of local angiogenic activity. Although statistically significant, the degree of correlation was only modest and there were several data points spread out around the regression line. This finding is consistent with a recent report in which tumor uptake of ^{18}F-galacto-RGD correlated to α_v integrin levels quantified by Western blots, but with considerable scattering of data (25). As previously discussed, this report suggests that tumor uptake of RGD radiotracers is not determined solely by local $\alpha_v\beta_3$ integrin levels but may also be influenced by nonspecific factors such as tissue perfusion and vascular permeability (25). In addition, it has recently been shown that evaluation of uptake at a single time point may be less accurate for assessing levels of tissue integrin expression than are more detailed dynamic kinetic studies and that quantification of integrin expression by SDS-PAGE/autoradiography may allow a more positive correlation with RGD tracer uptake levels than can Western blotting (14). Nevertheless, our observation of a significant

correlation between tumor glucosamino [99mTc-D-c(RGDfK)] uptake and α_v integrin expression after antiangiogenesis therapy offers encouragement for the potential of convenient [99mTc]-based scintigraphy for angiogenesis imaging.

CONCLUSION

Glucosamino [99mTc-D-c(RGDfK)] is a promising novel [99mTc]-labeled RGD tracer with favorable in vivo biokinetics and imaging properties that may allow noninvasive assessment of tumor integrin expression and response to antiangiogenic therapeutics. Because of the high availability and excellent imaging characteristics of [99mTc], glucosamino [99mTc-D-c(RGDfK)] may be an attractive alternative to halogenated RGD peptide radiotracers for angiogenesis-imaging research.

REFERENCES

1. Ruoslahti E. Specialization of tumour vasculature. *Nat Rev Cancer*. 2002; 2:83–90.
2. Hood JD, Cheresh DA. Role of integrins in cell invasion and migration. *Nat Rev Cancer*. 2002;2:91–100.
3. Felding-Habermann B. Integrin adhesion receptors in tumor metastasis. *Clin Exp Metastasis*. 2003;20:203–213.
4. Brooks PC, Clark RA, Cheresh DA. Requirement of vascular integrin $\alpha_v\beta_3$ for angiogenesis. *Science*. 1994;264:569–571.
5. Ellis LM, Liu W, Ahmad SA, et al. Overview of angiogenesis: biological implications for antiangiogenic therapy. *Semin Oncol*. 2001;28:94–104.
6. Brooks PC, Montgomery AM, Rosenfeld M, et al. Integrin alpha(v)beta 3 antagonists promote tumor regression by inducing apoptosis of angiogenic blood vessels. *Cell*. 1994;79:1157–1164.
7. Arap W, Pasqualini R, Ruoslahti E. Cancer treatment by targeted drug delivery to tumor vasculature in a mouse model. *Science*. 1998;279:377–380.
8. Hood JD, Bednarski M, Frausto R, et al. Tumor regression by targeted gene delivery to the neovasculature. *Science*. 2002;296:2404–2407.
9. Ruoslahti E, Pierschbacher MD. New perspectives in cell adhesion: RGD and integrins. *Science*. 1987;238:491–497.
10. Aumailley M, Gurrath M, Muller G, et al. Arg-Gly-Asp constrained within cyclic pentapeptides: strong and selective inhibitors of cell adhesion to vitronectin and laminin fragment P1. *FEBS Lett*. 1991;291:50–54.
11. Haubner R, Wester HJ, Reuning U, et al. Radiolabeled alpha(v)beta3 integrin antagonists: a new class of tracers for tumor targeting. *J Nucl Med*. 1999;40:1061–1071.
12. Haubner R, Wester HJ, Burkhart F, et al. Glycosylated RGD-containing peptides: tracer for tumor targeting and angiogenesis imaging with improved biokinetics. *J Nucl Med*. 2001;42:326–336.
13. Haubner R, Wester HJ, Weber WA, et al. Noninvasive imaging of $\alpha_v\beta_3$ integrin expression using [18F]-labeled RGD-containing glycopeptide and positron emission tomography. *Cancer Res*. 2001;61:1781–1785.
14. Zhang X, Xiong Z, Wu Y, et al. Quantitative PET imaging of tumor integrin {alpha}v{beta}3 expression with [18F]-FRGD2. *J Nucl Med*. 2006;47:113–121.
15. Chen X, Park R, Hou Y, et al. MicroPET imaging of brain tumor angiogenesis with [18F]-labeled PEGylated RGD peptide. *Eur J Nucl Med Mol Imaging*. 2004;31:1081–1089.
16. Chen X, Park R, Shahinian AH, Bading JR, Conti PS. Pharmacokinetics and tumor retention of [125I]-labeled RGD peptide are improved by PEGylation. *Nucl Med Biol*. 2004;31:11–19.
17. Su ZF, Liu G, Gupta S, et al. In vitro and in vivo evaluation of a technetium-99m-labeled cyclic RGD peptide as a specific marker of $\alpha_v\beta_3$ integrin for tumor imaging. *Bioconjug Chem*. 2002;13:561–570.
18. Janssen ML, Oyen WJ, Dijkgraaf I, et al. Tumor targeting with radiolabeled $\alpha_v\beta_3$ integrin binding peptides in a nude mouse model. *Cancer Res*. 2002;62:6146–6151.
19. Haubner R, Bruchertseifer F, Bock M, Kessler H, Schwaiger M, Wester HJ. Synthesis and biological evaluation of a [99mTc]-labelled cyclic RGD peptide for imaging the $\alpha v\beta 3$ expression. *Nuklearmedizin*. 2004;43:26–32.
20. Lee BC, Sung HJ, Song SH, et al. Synthesis of technetium-99m labeled glucosaminoAsp-Lys-Arg-Gly-Asp-D-Phe as a potential tumor imaging agent [abstract]. *J Labelled Compds Radiopharm*. 2003;46(suppl):S106.
21. Gutman M, Sofer D, Lev-Chelouche D, Merimsky O, Klausner JM. Synergism of tumor necrosis factor-alpha and melphalan in systemic and regional administration: animal study. *Invasion Metastasis*. 1997;17:169–175.
22. Horwitz SB. Taxol (paclitaxel): mechanisms of action. *Ann Oncol*. 1994; 5(suppl):S3–S6.
23. Myoung H, Hong SD, Kim YY, Hong SP, Kim MJ. Evaluation of the anti-tumor and anti-angiogenic effect of paclitaxel and thalidomide on the xenotransplanted oral squamous cell carcinoma. *Cancer Lett*. 2001;163:191–200.
24. Hosten B, Challuau D, Gil S, et al. Recombinant interleukin-2 pre-treatment increases anti-tumor response to paclitaxel by affecting lung P-glycoprotein expression on the Lewis lung carcinoma. *Anticancer Drugs*. 2006;17:195–199.
25. Haubner R, Weber WA, Beer AJ, et al. Noninvasive visualization of the activated alphavbeta3 integrin in cancer patients by positron emission tomography and [18F]galacto-RGD. *PLoS Med*. 2005;2:244–252.